

ORIGINAL RESEARCH COMMUNICATION

# Thioredoxin-Like Protein 2 Is Overexpressed in Colon Cancer and Promotes Cancer Cell Metastasis by Interaction with Ran

Yuanyuan Lu,<sup>1,\*</sup> Xiaodi Zhao,<sup>1,\*</sup> Kai Li,<sup>1,\*</sup> Guanhong Luo,<sup>1,\*</sup> Yongzhan Nie,<sup>1</sup> Yongquan Shi,<sup>1</sup> Yi Zhou,<sup>1,2</sup> Gui Ren,<sup>1</sup> Bin Feng,<sup>1</sup> Zhenxiong Liu,<sup>1</sup> Yan Pan,<sup>1</sup> Ting Li,<sup>1</sup> Xuegang Guo,<sup>1</sup> Kaichun Wu,<sup>1</sup> Antonio Miranda-Vizuete,<sup>3</sup> Xin Wang,<sup>1</sup> and Daiming Fan<sup>1</sup>

## Abstract

**Aims:** Our previous work identified thioredoxin-like protein 2 (Txl-2) as the target of the monoclonal antibody MC3 associated with colon cancer, but its underlying mechanisms remain poorly understood. Txl-2, a novel thioredoxin (Trx) and nucleoside diphosphate kinase family member, is alternatively spliced and gives rise to three different Txl-2 isoforms. In this study, Txl-2 expression in colon cancer, differential functions for Txl-2 isoforms in cell invasion and metastasis, and the downstream signaling were investigated. **Results:** Txl-2 expression was elevated in colon cancer tissues compared to normal colonic tissues, with a high correlation between the histological grade and prognosis. Knockdown of Txl-2 expression significantly inhibited cancer cell motility, and the invasive and metastatic abilities of colon cancer cells. Interestingly, Txl-2 isoforms showed differential effects on cancer cell invasion and metastasis. Cell invasion and metastasis were significantly promoted by Txl-2b but inhibited by Txl-2c, while no obvious effect was observed for Txl-2a. Furthermore, a direct interaction was identified between Txl-2b and Ran, a Ras-related protein, by yeast two-hybrid assay and coimmunoprecipitation. PI3K pathway was found to be a major pathway mediating Txl-2b induced tumor invasion and metastasis. **Innovation:** The current study provides a novel biomarker and target molecule for the diagnosis and treatment of colon cancer and provides a novel paradigm to understand how alternative splicing functions in human cancer. **Conclusion:** Our findings demonstrate an elevated Txl-2 expression in colon cancer and that Txl-2b promotes cell invasion and metastasis through interaction with Ran and PI3K signaling pathway. *Antioxid. Redox Signal.* 19, 899–911.

## Introduction

COLORRECTAL CANCER (CRC) is the fourth most common cancer in men and the third in women worldwide (7). Identification of novel biomarkers specific to CRC is essential for cancer screening, patient stratification, and prognosis prediction. Importantly, these biomarkers can serve as targets for developing novel cancer therapeutics (11). In this context, we have previously identified thioredoxin-like protein 2 (Txl-2) as the target of the monoclonal antibody MC3 that we have generated for the detection of colon cancer (25).

Txl-2, a member of the thioredoxin (Trx) and nucleoside diphosphate kinase (NDP<sub>k</sub>) family, was cloned and characterized in 2003 (37). It is mainly expressed in testis, and at lower levels in lung and brain, while more ubiquitously expressed at very low levels in other tissues (37). While Txl-2 function in cancer remains largely unknown, other Trx family members have been reported to be critical in the regulation of tumor development and progression. For instance, Trx-1 is overexpressed in a number of human primary tumors, including lung, colorectal, and cervical cancers and leukemia (23). Specifically, an increased expression of Trx-1 in CRC has

<sup>1</sup>State Key Laboratory of Cancer Biology, Xijing Hospital of Digestive Diseases, Fourth Military Medical University, Xi'an, China.

<sup>2</sup>Tianjin Union Medicine Centre, Tianjin, China.

<sup>3</sup>Instituto de Biomedicina de Sevilla (IBiS), Hospital Universitario Virgen del Rocío/CSIC/Universidad de Sevilla, Seville, Spain.

\*These authors contributed equally to this work.

### Innovation

Thioredoxin (Trx) system has been increasingly linked to cancer malignant phenotypes in the recent years. In this work, we provide further evidence to this scenario by reporting another Trx family member thioredoxin-like protein 2 (Txl-2), which is upregulated in colon cancer with a strong correlation with patient prognosis. Txl-2 was initially identified as the target of the monoclonal antibody MC3, previously isolated in our laboratory, which detects colon cancer with high sensitivity and specificity. We demonstrate now that the most abundant isoform Txl-2b promotes colon cancer metastasis. Our studies show that interaction between Txl-2b isoform and the small GTPase family member Ran mediates colon cancer cell invasion and metastasis *via* phospho-Akt activation and induction of matrix metalloproteinases expression. Taken together, our data uncover Txl-2 as a novel biomarker and target molecule for human cancer and offers a novel mechanism of how Trx family members regulate metastasis.

been shown to be associated with poor prognosis in patients with liver metastasis (30). We have recently demonstrated an increased expression of Txl-2 in colon cancer (25), but its specific role in colon cancer and the underlying mechanisms are still unknown.

It is well-recognized that mRNA splicing can lead to production of protein isoforms with oncogenic properties (32). Three different isoforms have been identified for Txl-2, including full length Txl-2 (Txl-2a), Txl-2b (splicing variant lacking exons 1 and 5), and Txl-2c (splicing variant lacking exons 1, 4, and 5) (25, 37). Of these, Txl-2b was upregulated in colon cancer tissues compared with normal mucosa, while Txl-2c was almost exclusively present in colon cancer tissues, and full length Txl-2 seldom occurred in both normal mucosa and colon cancer tissues (25). Thus, it would be interesting to investigate whether these three transcript variants show differential effects on the functional properties of colon cancer cells.

The ability to invade tissues and metastasize to other sites is one of the most critical clinical parameters in predicting the progression of cancer to a more aggressive phenotype. We hypothesized that Txl-2 may mediate colon cancer progression and especially metastasis based on the following reasons. First, it is well established that the cytoskeleton plays a crucial role in tumor metastasis (15). Txl-2b was found to possess intrinsic microtubule binding capability, and therefore, might be a novel regulator of microtubule physiology (37). Second, Txl-2, also named nm23-H9, belongs to the NDPk family that has been extensively studied in regard to their roles in cancer metastasis. Ten genes belonging to the NDPk family have been identified in humans (4). Among them, the nm23-H1 was the first identified metastasis suppressor gene (5), whereas nm23-H4, nm23-H6, and nm23-H7, were found to be overexpressed in gastric and colon cancer (38). However, the role of Txl-2 (nm23-H9) in colon cancer metastasis remains largely unknown.

In the present study, we examined the Txl-2 expression in 243 cases of colon cancer tissues and found that overexpression of Txl-2 strongly correlated with the histological grade and prognosis of colon cancer patients. Knockdown of Txl-2 expression significantly inhibited the invasive and

metastatic abilities of colon cancer cells. The differential effects of each Txl-2 isoform on cancer cell invasion and metastasis were further investigated. Overexpression of the most abundant isoform Txl-2b (88%) can promote cancer cell invasion and metastasis. Txl-2b harbors a regulator of chromosome condensation-1 (RCC1) motif which is absolutely required for a newly discovered interaction with Ran. We further explored the downstream signaling events that participated in the Txl-2b-Ran mediated invasion and metastasis.

### Results

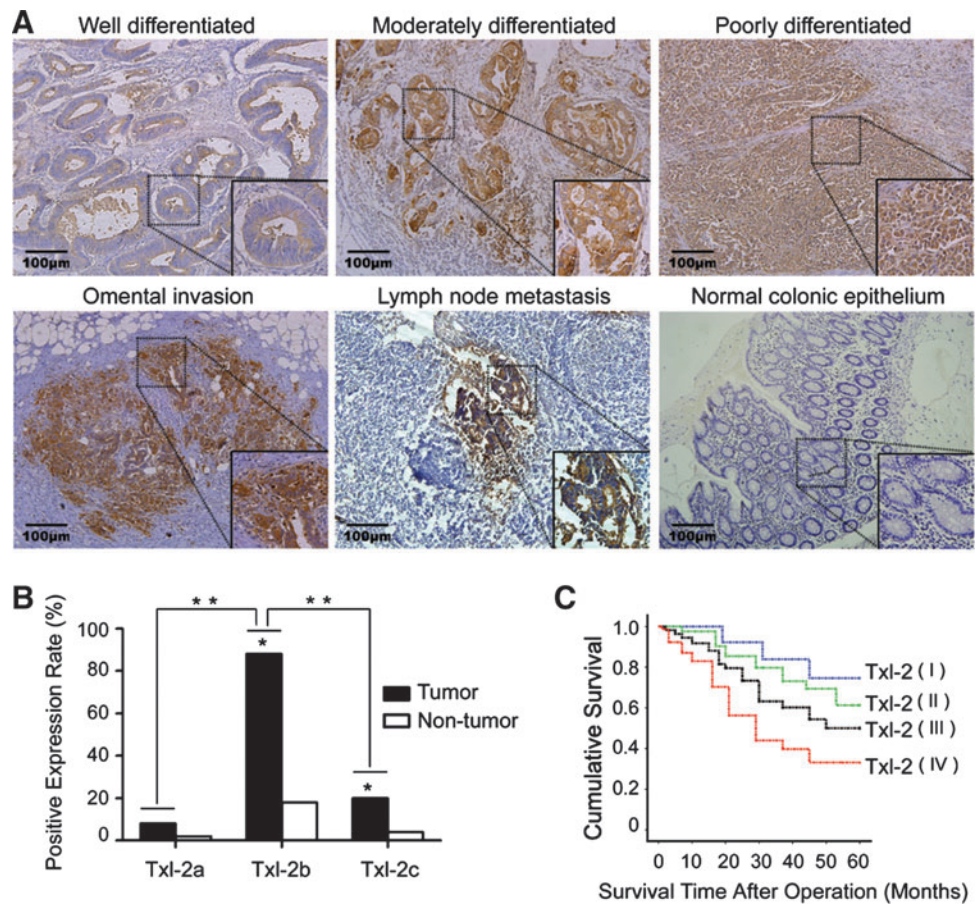
#### *Upregulation of Txl-2 in colon cancer correlates with tumor staging and patient survival*

The expression of Txl-2 in human colon cancer tissues and adjacent nontumorous tissues was examined in 243 colon cancer patients. We found that Txl-2 expression was increased in colon cancer cells compared to adjacent nontumorous tissues, and normal colonic epithelium (Fig. 1A), and the increased expression was significantly correlated with the degrees of cancer cell differentiation (Table 1,  $p=0.019$ ). As shown in Table 1, the increased Txl-2 expression also correlated with tumor stages consisting of tumor size (T) ( $p<0.001$ ), lymph node invasion (N) ( $p<0.001$ ), and distant metastasis (M) ( $p=0.022$ ). To determine whether Txl-2 isoforms have differential expression rates, a semiquantitative reverse transcription polymerase chain reaction (RT-PCR) analysis was performed in 50 pairs of colon cancer samples using the method we reported previously (25). We found that Txl-2b was the most frequently presented Txl-2 isoform in tumor tissues (88%, 44/50), as compared to Txl-2a (8%, 4/50,  $p<0.001$ ) and Txl-2c (20%, 10/50,  $p<0.001$ ) (Fig. 1B). These results supported our previous findings that the total Txl-2 mRNA level was elevated in colon cancer tissues compared with paracancerous tissues and adjacent normal tissues in a relatively small number of patients (25). Furthermore, we investigated whether Txl-2 expression can be an independent prognostic factor. In general, the mean follow-up time of the patients with colon cancer was 41.8 months with a median value of 50 months. The 5-year survival rate of the 243 patients was 47%. Importantly, the survival rates based on cumulated survival and survival time after operation were inversely correlated with Txl-2 expression as shown by the Kaplan–Meier postoperative survival curve (Fig. 1C, log-rank test:  $p<0.001$ ). Further multivariate analysis demonstrated Txl-2 expression as an independent prognostic factor (Table 2). Adjusted hazard ratio (HR) was set to 1.00 in the Txl-2 negative (I) expression group; the adjusted HR of weak positive (II), moderate positive (III), and strong positive (IV) groups were 1.74, 1.96, and 3.02, respectively. All these data pointed to an important role for Txl-2 as an independent prognostic factor for patients with colon cancer.

#### *Depletion of Txl-2 inhibits in vitro invasive and in vivo metastatic properties of colon cancer cells*

To explore the impact of Txl-2 on colon cancer invasion and metastasis, we knocked down Txl-2 expression in the SW620 colon cancer cell line which has a high metastatic potential (19) by using Txl-2-specific siRNA targeted to the overlapping sequences of three Txl-2 isoforms, aiming to knock down simultaneously the expression of all Txl-2 isoforms. Two Txl-2

**FIG. 1.** TxI-2 expression in colon cancer tissues and its association with patients' survival. **(A)** Results from immunohistochemical staining. Upper row: well differentiated (*left panel*), moderately differentiated (*middle panel*), and poorly differentiated colon cancer tissues (*right panel*); lower row: moderately differentiated cancer tissues with omental invasion (*left panel*), metastatic site in lymph node (*middle panel*), and normal colonic epithelium (*right panel*). Brown color represents a positive staining for thioredoxin-like protein 2 (TxI-2). **(B)** Positive expression rates of the three TxI-2 splicing variants from tumor ( $n=50$ ) and nontumor ( $n=50$ ) samples as determined by reverse transcription polymerase chain reaction (RT-PCR).  $*p < 0.05$ ,  $**p < 0.01$ . **(C)** Kaplan-Meier postoperative survival curve by TxI-2 expression. (I) TxI-2 negative expression group; (II) TxI-2 weak positive expression group; (III) TxI-2 moderate positive expression group; (IV) TxI-2 strong positive expression group.



siRNA expression vectors named pSilencer TxI-2 (#si1 and #si2) were constructed, and the knock down efficacy was compared based on TxI-2 expression using specific TxI-2 antibodies able to recognize the three isoforms (37). We found that SW620-TxI-2si1 cells were able to inhibit TxI-2 expression by 3.1-fold compared to the scrambled control ( $p=0.0004$ ), whereas SW620-TxI-2si2 did not result in significant TxI-2 downregulation (Fig. 2A). To test the impact of TxI-2 on cell migration, we performed a wound healing assay by using SW620-TxI-2si1. As shown in Figure 2B, TxI-2 downregulated cells exhibited longer healing time than the control cells. Moreover, as compared to control cells, the TxI-2 downregulated cells showed a reduced cell invasive ability in the Transwell invasion assay (Fig. 2C). Specifically, SW620-TxI-2si1 cells showed the strongest inhibition of cell invasion over the SW620-Scrambled control cells (2.85-fold,  $p=0.006$ ). Moreover, these SW620-TxI-2si1 cells significantly reduced the number of colonies in a colony formation assay in soft agar relative to SW620-Scrambled control (2.81-fold,  $p=0.006$ , Fig. 2D). Next, tail vein metastatic assay in nude mice was conducted to examine the metastatic ability of SW620-TxI-2si1 cells *in vivo*. Notably, compared with SW620-Scrambled control, *i.v.* inoculation of SW620-TxI-2si1 cells led to a significant reduction of visible tumors in liver and lung, which correlated with a lower number of metastasis loci ( $p < 0.05$ ,  $p < 0.01$ , respectively, Fig. 2E). In addition, mice inoculated with SW620-TxI-2si1 cells presented a prolonged survival time with the median survival time of 35.0 days compared with 26.0 days of the mice injected with SW620-Scrambled control cells

( $p < 0.001$ , Fig. 2F). Together, these studies demonstrate that TxI-2 promotes invasion and metastasis of colon cancer cells.

*Differential effects of TxI-2 isoforms on colon cancer cell invasion and metastasis*

To delineate the distinctive functions of the three TxI-2 isoforms (Fig. 3A) (25, 37), expression constructs of each TxI-2 transcript variant (pEGFP-N3-TxI-2a, b, and c) were stably transfected into LoVo cells, a cell line lacking endogenous TxI-2 expression. The stable expression of the different TxI-2 isoforms was confirmed by Western blot and immunostaining with anti-GFP antibodies by showing TxI-2a, b, and c-EGFP fusion protein expression, respectively (Fig. 3B). By using these stably transfected cells, we investigated the differential effects of the TxI-2 isoforms on cell invasion (Fig. 3C) and soft agar colony formation (Fig. 3D) that we had observed for TxI-2 siRNA. Among the three TxI-2 isoforms, the strongest stimulatory effect was seen for TxI-2b. In particular, enforced expression of TxI-2b-EGFP in LoVo cells increased the cellular invasion (1.87-fold,  $p=0.002$ , Fig. 3C) and increased anchorage independent growth in soft agar (2.10-fold,  $p=0.07$ , Fig. 3D). Interestingly, no obvious change was observed for cells transfected with TxI-2a-EGFP, while a reverse effect was noted for cells with TxI-2c-EGFP. Cells with TxI-2c-EGFP significantly suppressed the cellular invasion (2.59-fold,  $p=0.004$ , Fig. 3C) and the colony growth (2.38-fold,  $p=0.01$ , Fig. 3D) when compared with the control cell lines, respectively. These findings were further supported by *in vivo*

TABLE 1. STATISTICAL RESULTS OF IMMUNOHISTOCHEMICAL ASSAY

	Expression level of Txl-2					p
	n	I	II	III	IV	
Total	243	13	42	110	78	
Age (years)						0.94
≤60	109	7	18	48	36	
>60	134	6	24	62	42	
Gender						0.259
Men	125	4	20	59	42	
Women	118	9	22	51	36	
Differentiation						0.019 <sup>a</sup>
Poor	81	2	10	37	32	
Moderate	107	5	19	50	33	
High	55	6	13	23	13	
TNM staging						
T T1	8	1	3	3	1	<0.001 <sup>a</sup>
T2	51	6	13	19	13	
T3	102	4	21	49	28	
T4	82	2	5	39	36	
N N0	86	9	24	31	22	0.001 <sup>b</sup>
N(1–2)	157	4	18	79	56	
M M0	205	12	38	95	60	0.022 <sup>b</sup>
M1	38	1	4	15	18	

<sup>a</sup>p value when expression levels were compared using Kruskal-Wallis test.

<sup>b</sup>p value when expression levels were compared using Mann-Whitney test.

TNM, tumor-node-metastasis staging classification system. From National Comprehensive Cancer Network (NCCN) guidelines. Available at: [www.nccn.org](http://www.nccn.org) (Accessed on Mar 15, 2012).

metastatic assay. Inoculation of Txl-2b-EGFP transfected cells through tail vein led to a significant increase in visible tumors in liver and lung which also correlated to the number of metastasis loci (both  $p < 0.01$ ). In contrast, Txl-2c-EGFP transfected cells resulted in less visible tumors in liver and lung (both  $p < 0.01$ ,

TABLE 2. MULTIVARIATE ANALYSIS BASED ON A COX PROPORTIONAL-HAZARDS MODEL

	HR <sup>a</sup>	95% Confidence interval	p
T			
T1	1.00	—	—
T2	0.485	0.16–1.44	0.19
T3	1.557	0.56–4.30	0.39
T4	4.914	1.75–13.77	0.002
N			
N0	1.00	—	—
N1-2	2.99	2.08–4.30	<0.001
Txl-2 expression			
I	1	—	—
II	1.74	0.74–4.09	0.20
III	1.96	0.87–4.40	0.10
IV	3.02	1.34–6.81	0.008

Multivariate analysis was used to evaluate whether Txl-2 expression is an independent prognostic factor for colon cancer patients.

<sup>a</sup>Adjusted HR was set to 1.00 in the Txl-2 negative (I) expression group.

T, extent of the tumor; N, nearby (regional) lymph nodes; from NCCN guidelines. Available at: [www.nccn.org](http://www.nccn.org) (Accessed on Mar 15, 2012).

HR, hazard ratio; Txl-2, thioredoxin-like protein 2.

Fig. 3E). Interestingly, mice inoculated with Txl-2b-EGFP cells presented a shortened survival time with a median survival time of 22.0 days compared to the 30.0 days of the mock control ( $p < 0.001$ , Fig. 3F), while Txl-2c-EGFP inoculation prolonged the median survival time to 35.0 days ( $p < 0.05$ , Fig. 3F). These results demonstrate that the most abundant isoform Txl-2b exerts the major effects on promoting cancer cell invasion and metastasis, whereas Txl-2c has an inhibitory role.

#### The Trx domain of Txl-2b is essential for inducing invasion and metastasis of colon cancer cells

Txl-2 is composed of an N-terminal Trx domain followed by one NDPk domain, both separated by an interface domain (25, 37). To investigate whether both Trx and NDPk domains modulate the functional properties of Txl-2 isoforms in cancer cell invasion and metastasis, we analyzed the role of the Trx domain by generating a redox inactive Txl-2b variant (Txl-2b<sup>CS</sup>) in which the cysteine residues at the active site of the Trx domain were replaced by serine residues (W<sub>CGPC</sub>→W<sub>SGPS</sub>) (Fig. 4A). Similarly, we generated a NDPk domain inactive variant Txl-2b<sup>H217P</sup> by replacing the NDPk active site histidine residue to a phenylalanine residue at amino acid position 217 (Fig. 4A). In total, we generated 4 variants consisting of wild-type Txl-2b, Txl-2b with a mutated Trx domain (Txl-2b<sup>CS</sup>), Txl-2b with a mutated NDPk domain (Txl-2b<sup>HP</sup>), and Txl-2b with both Trx and NDPk domains mutated (Txl-2b<sup>DM</sup>) (Fig. 4A). Notably, overexpression of the variant with the mutated Trx domain Txl-2b<sup>CS</sup>, but not the mutated NDPk domain Txl-2b<sup>HP</sup>, strongly inhibited Txl-2b induced invasion of colon cancer cells, as compared to the wild-type Txl-2b overexpressing LoVo cells (2.47-fold,  $p = 0.002$ , Fig. 4B). Furthermore, overexpression of Txl-2b<sup>CS</sup> also impaired the colonization of colon cancer cells in soft agar ( $p = 0.01$ , Fig. 4C). No enhancement of the phenotype was observed when overexpressing the variant with both active sites mutated Txl-2b<sup>DM</sup> in comparison to Txl-2b<sup>CS</sup>. These results indicate that the Trx domain in Txl-2b plays a prominent role at inducing invasion and metastasis of colon cancer cells and that this effect is redox dependent.

#### Txl-2b interacts with the small GTPase Ran

Next, to gain deeper insight into the molecular mechanisms mediating Txl-2 function, we set to identify potential binding partners of Txl-2. A search in the PROSITE database ([www.expasy.org/prosite/](http://www.expasy.org/prosite/)) (40) identified an RCC1 motif (MCSGSPSHLLIL) between residues 222 and 232 of Txl-2 (37). RCC1 is a chromatin-bound guanine nucleotide exchange factor (GEF) for Ran, a Ras-related protein (34, 35). To confirm whether Ran is a Txl-2 binding partner, we performed a yeast two-hybrid assay. As shown in Figure 5A, an interaction was detected for Txl-2b and Ran but not for Txl-2a, Txl-2c, and the negative control. To check whether Txl-2b interacts with Ran through the predicted RCC1 signature, we generated a vector expressing a Txl-2b variant with a deletion of the RCC1 signature. As shown in Figure 5A, the interaction Txl-2b<sup>ARCC1</sup> and Ran was lost in the yeast two-hybrid assay. To examine the interaction between Ran and Txl-2 *in vivo*, we co-transfected HA-Ran and the three Flag-Txl-2 isoforms plus the Txl-2b<sup>ARCC1</sup> mutant into 293T cells and determined whether Flag antibodies immunoprecipitate HA-Ran. The results show that only Txl-2b interacts with Ran, whereas Txl-2b<sup>ARCC1</sup> failed to coimmunoprecipitate Ran, demonstrating

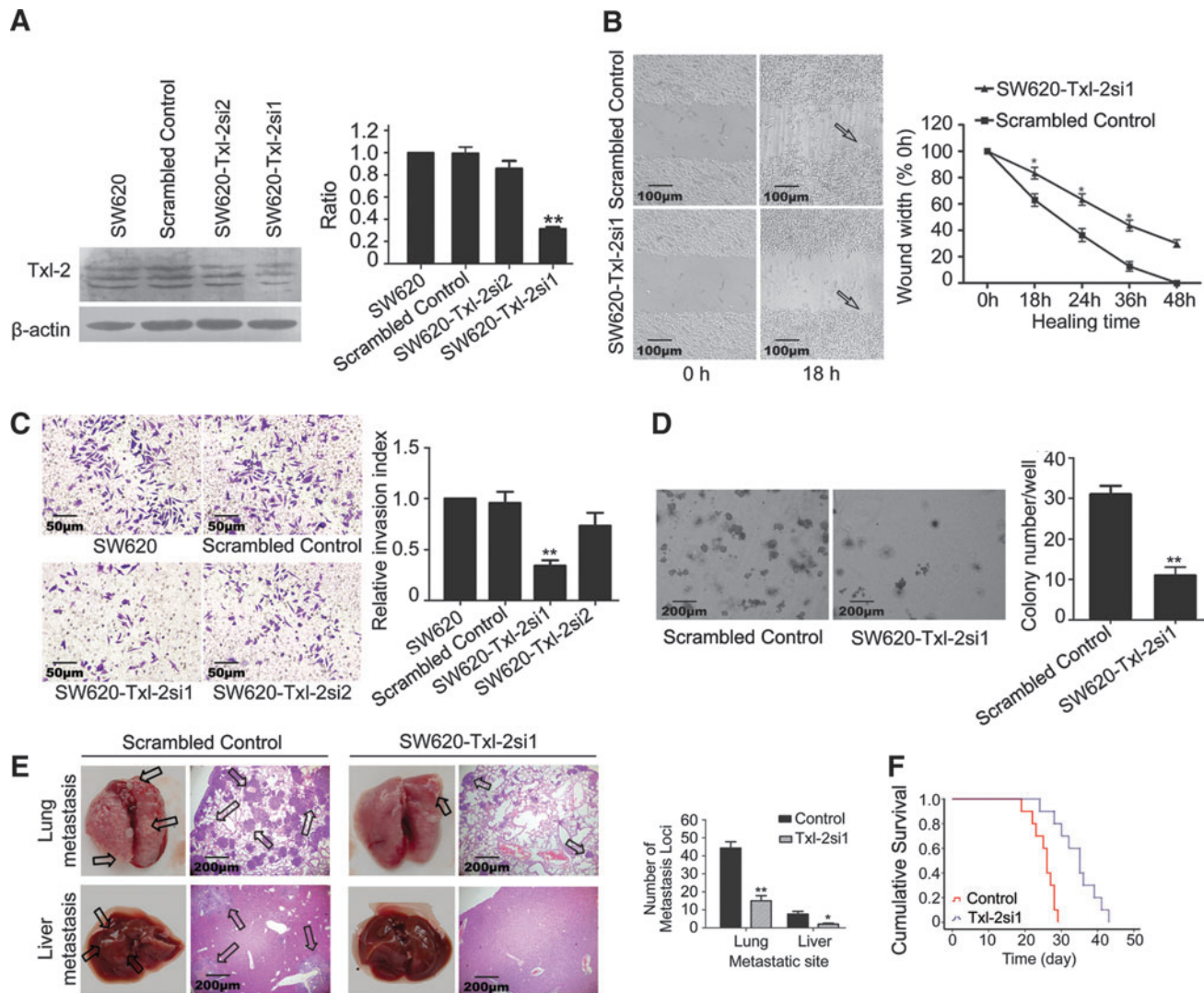


**FIG. 2. Knockdown of Txl-2 inhibits motility, invasion, and *in vivo* metastatic properties of colon cancer cells.** (A) Txl-2 was knocked down in SW620 Cells with two different Txl-2 siRNA expression vectors and Txl-2 downregulation was evaluated by Western blot. The sum of the densitometric units of all the three bands was counted when the positive Txl-2 expression was quantified. (B) Scratch wounds were made in monolayer cultures of cells after plating (*left panel*). A slower closure of the wound in the SW620-Txl-2si culture from 1 to 48 h based on the wound width is shown in the graph (*right*), as compared to the controls. The wound margins are indicated by *arrows*. (C) Tumor cell invasion capacity was measured with Transwell chambers. Representative image fields of invasive cells on the membrane are shown. Data are represented as normalized invasion (invasion index) relative to the control cells. (D) The ability of stably transfected cells to grow in an anchorage independent environment was assessed by the soft agar assay. The numbers of colonies formed on day 5 were determined. All above images shown are representative of three independent experiments. (E) Metastatic potential *in vivo* ( $n=8$ ). H&E staining of lungs and livers was performed in samples from mice that received intravenous tail injections of SW620-Txl-2si1 and scrambled control cells, respectively, with metastatic loci marked by *arrows*. Number of metastatic loci in lung and liver were counted (*middle*). (F) Kaplan–Meier survival curves show that knock down of Txl-2 markedly prolonged the survival of the mice bearing SW620 tumors ( $n=10$ ). \* $p<0.05$ , \*\* $p<0.01$ . To see this illustration in color, the reader is referred to the web version of this article at [www.liebertpub.com/ars](http://www.liebertpub.com/ars)

that Txl-2b interacts with Ran *via* its RCC1 signature (Fig. 5B). We also confirmed the interaction between Txl-2b and Ran by coimmunoprecipitation in SW620 cells (Fig. 5C). To further sustain this interaction, we performed immunofluorescence and confocal microscopy showing that Ran and Txl-2 colocalize in the cytoplasm of colon cancer cells (Fig. 5D) and colonic tissues (Fig. 5E). Paired immunostaining analysis also revealed a strong correlation between Txl-2 and Ran expression (Table 3). These results provided strong evidence for the

role of Txl-2b in modulating colon cancer cell metastasis through binding to the small GTPase Ran.

#### *Phospho-Akt mediates the Txl-2b-Ran-matrix metalloproteinase signaling induced tumor cell invasion*

Ran is a well-recognized downstream effector of the PI3K signaling pathway that mediates invasion and metastasis of

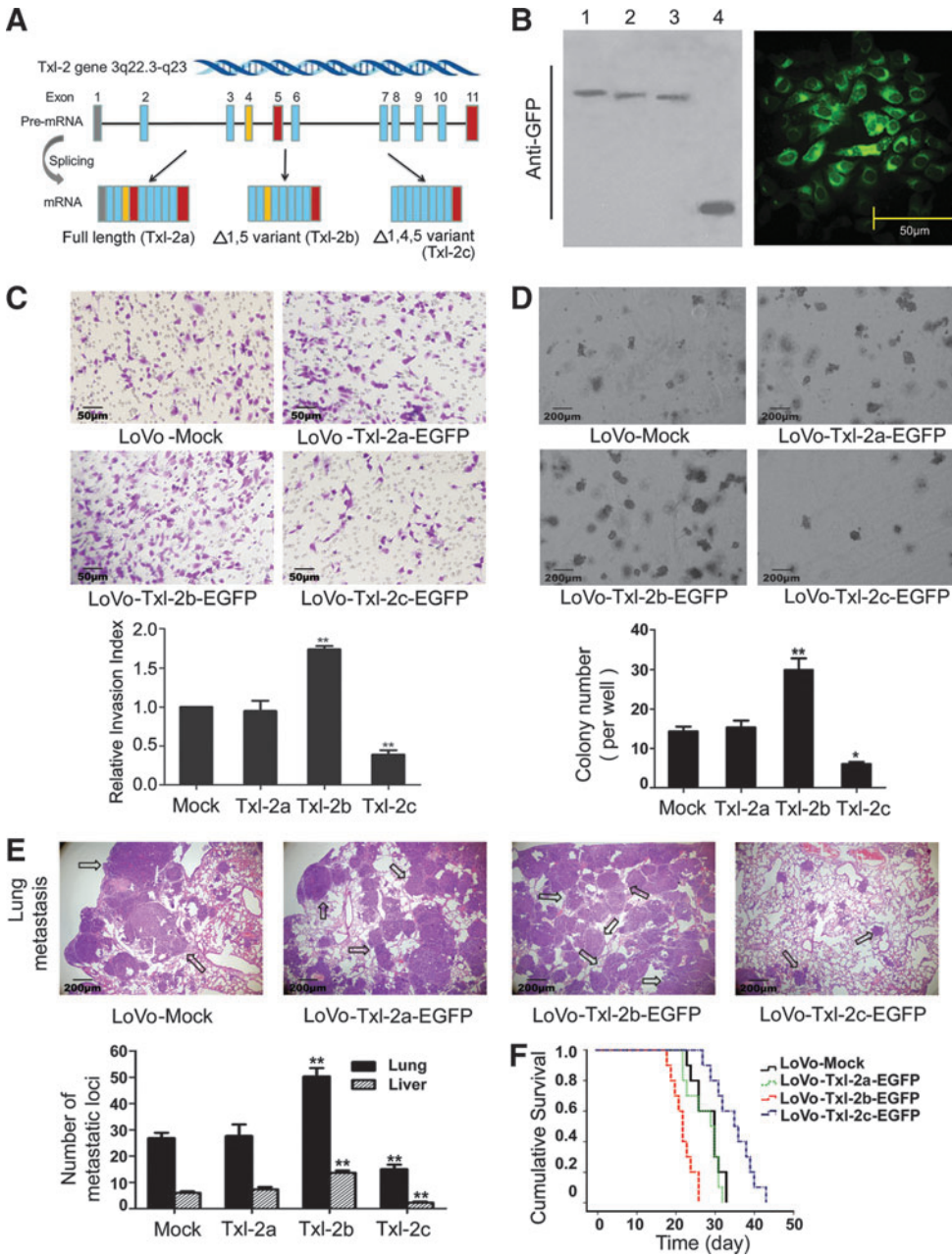


**FIG. 3. Txl-2 splicing variants produce differential effects on cell invasion and metastasis.** (A) Schematic representation of the three Txl-2 splicing variants (Txl-2a, b, and c). (B) LoVo cells stably transfected with pEGFP-N3-Txl-2a, b, and c. Txl-2 isoform-EGFP fusion proteins in LoVo cells were detected with the GFP antibody (lane 1 to 3). Lane 4 is the empty vector transfected cells producing only GFP as the negative control. The accompanying image shows the green fluorescence from LoVo cells transfected with the pEGFP-N3-Txl-2b construct. Overexpression of the three Txl-2 isoform-EGFP fusion proteins in LoVo cells resulted in different effects evaluated by *in vitro* invasion assay (C) and soft agar colonization (D). The results were the mean  $\pm$  SEM from three independent experiments. (E) *in vivo* tail vein metastasis assay. Metastatic loci are denoted by arrows. (F) Kaplan–Meier survival curves show that overexpression of Txl-2b-EGFP markedly shortened survival of the mice bearing LoVo tumor ( $n=10$ ). \* $p < 0.05$ , \*\* $p < 0.01$  relative to vector control transfected cells.

cancer cells (20). Thus, the involvement of Txl-2b interaction with Ran in cancer cell metastasis and the PI3K pathway was further investigated. We found that SW620 cells with decreased levels of Txl-2 showed a lack of Akt activation as detected by a specific antibody to phosphoserine 473 of Akt (Fig. 6A), whereas overexpression of Txl-2b resulted in an elevated Akt activation (Fig. 6B). Interference of Txl-2b and Ran interaction by deleting the RCC1 signature in Txl-2b strongly abolished the enhanced invasive potential of Txl-2b overexpressing LoVo cells, accompanied by a decrease in the levels of matrix metalloproteinase (MMP) and phospho-Akt (Ser 473) (Fig. 6B, D). The same effect was also noticed when downregulating Ran expression by siRNA in Txl-2b transfected cells (Fig. 6D, E, and Supplementary Methods and Suppl. Fig. S1; Supplementary Data are available online at [www.liebertpub.com/ars](http://www.liebertpub.com/ars)), suggesting that Txl-2b-Ran inter-

action plays a pivotal role in mediating the Txl-2b induced cancer cell invasion and metastasis. Furthermore, Txl-2b induced cancer cell invasion was significantly inhibited by the PI3K signaling inhibitor LY294002 (10  $\mu$ M) with an average inhibiting rate of 68.4% ( $p=0.02$ ), but not by the ERK pathway inhibitor U0126 (10  $\mu$ M) ( $p=0.46$ ) (Fig. 6D). Previous studies have reported that Trx family members regulate MMPs, which play key roles in tumor invasion and metastasis (13, 14, 31). To examine whether Txl-2 regulates MMP expression, we downregulated Txl-2 expression by siRNA in SW620 cells and MMP-2 and MMP-9 protein levels were determined by Western blot. We found that MMP-2 and MMP-9 were significantly inhibited in SW620 cells when Txl-2 levels are decreased (Fig. 6A). The MMP-2 and MMP-9 proteins secreted into the conditioned medium were also determined using gelatin zymography. The gelatinolytic activity of MMP-2 and

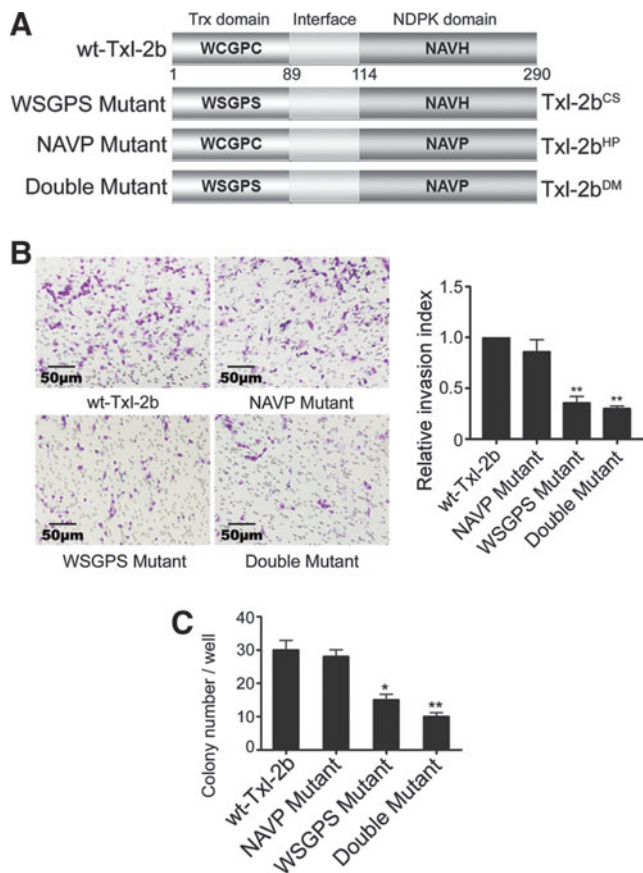


**FIG. 4. The Trx domain is essential for inducing invasion and metastasis of colon cancer cells.** (A) Schematic representation of Txl-2b isoforms harboring mutations in either the Trx domain active site WCGPC or the NDPk domain NAVH active site. Numbers below the wild type Txl-2b indicate the amino acid residues. (B) LoVo cells transfected with the different Txl-2b-EGFP mutant variants were subjected to an *in vitro* invasion assay. Relative invasion index represents fold change of the number of migrated cells relative to the cells transfected by wild-type Txl-2b. (C) Numbers of soft agar colony forming units were also counted. The results were the mean  $\pm$  SEM from three independent experiments. \* $p < 0.05$ , \*\* $p < 0.01$ . To see this illustration in color, the reader is referred to the web version of this article at [www.liebertpub.com/ars](http://www.liebertpub.com/ars)

MMP-9 was significantly reduced in Txl-2si1-transfected SW620 cells as compared to the parental and the scrambled controls (Fig. 6C). We further examined whether overexpression of three different Txl-2 isoforms in SW620 resulted in differential MMP-2 and MMP-9 expression. Indeed, Txl-2b-EGFP induced the strongest expression of MMP-2 and MMP-9 (Fig. 6B) as well as the highest gelatinolytic activity (Fig. 6C) compared to the other isoforms and the mock control. However, overexpression of Txl-2b-EGFP without the RCC1 signature (Txl-2b<sup>ARCC1</sup>-EGFP) did not affect the expression levels nor the activities of MMP-2 and MMP-9 (Fig. 6B, C), suggesting that Txl-2b regulates MMP-2 and MMP-9 through its interaction with Ran. Consistently, the Txl-2b induced cancer cell invasion phenotype was inhibited in a Transwell invasion assay when MMP-2 and MMP-9 neutralizing antibodies were added into the culture medium at the bottom of Transwell

(Fig. 6D). Western blot analysis further corroborated the inhibition of MMP2, MMP9, and Akt activation after cells were treated with the PI3K inhibitor (LY294002) and MMP neutralizing antibodies (anti-MMP-2, anti-MMP-9), respectively (Fig. 6E). These results suggest that the PI3K pathway mediates Txl-2b-Ran-MMP signaling in tumor cell invasion.

**Discussion**

In the present study, we demonstrate that Txl-2 plays a key role in colon cancer cell progression and metastasis. Txl-2 overexpression was significantly correlated with the degrees of cancer cell differentiation and tumor staging. More importantly, Txl-2 expression was inversely correlated with survival time of colon cancer patients. Taken together, our data suggest that Txl-2 could be a novel prognostic factor for patients with CRC. Normally, Txl-2 is predominantly expressed in testis and at much lower levels in other somatic tissues, while our previous study has identified Txl-2 in several cancer tissues (25). Therefore, Txl-2 might be a novel member of the cancer-testis antigens family (24), which is characterized by a restricted expression to testis germline cells in normal tissues and their expression being dysregulated in different tumor malignancies.

To explore its functions, we knocked down Txl-2 in the colon cancer cell line SW620, which has a high metastatic potential (19) and performed *in vitro* and *in vivo* functional studies showing that depletion of Txl-2 significantly inhibits the metastatic potential of colon cancer cells. Subsequently, the effects of the different Txl-2 isoforms on cancer cell invasion and metastasis were investigated. Interestingly, the most abundant isoform Txl-2b (88%) showed the strongest stimulatory effect on cellular invasion, anchorage independent growth in soft agar, and *in vivo* metastasis. Compared to Txl-2b, Txl-2a seemed to have little effect but, in contrast, Txl-2c played the opposite function on cancer cells. These results demonstrate that Txl-2b is the major isoform responsible for the Txl-2 function in cancer cell invasion and metastasis. As for Txl-2c, considering that it only appears along with Txl-2b (25), we deem it might function *via* a negative feedback manner for Txl-2b. Interestingly, alternative splicing is not a rare phenomenon involved in human pathology caused by Trx family. Differential isoforms of thioredoxin reductase 1 (TrxR1) were found in different malignancies and could be a valuable tool in the diagnostics and characterization of tumors (36). Isoform-specific modulation of tumor phenotypes was also reported in other well-studied oncogenic proteins, such as CD44, OPN and Survivin (6, 9, 41).

We investigated the role of the Trx and NDPK domains on the functional properties of Txl-2b by introducing inactivating mutations in the respective active sites of both domains. Notably, only the redox-inactive Trx domain, but not the mutated NDPK domain, strongly inhibited Txl-2b induced invasion and colonization of colon cancer cells, suggesting that the Trx domain plays a prominent role in its oncogenic properties of Txl-2b. The redox activity of Trx resides in the sequence of its conserved active site Cys-Gly-Pro-Cys (CGPC), which undergoes reversible oxidation of the two cysteine residues from a dithiol to a disulfide form (23). Several functions have been discovered for Trxs in human cancer, mostly dependent on its redox activity, including regulation of transcription factor activity, modulation of apoptosis, and regulation of cell motility, angiogenesis, and metastasis (23,

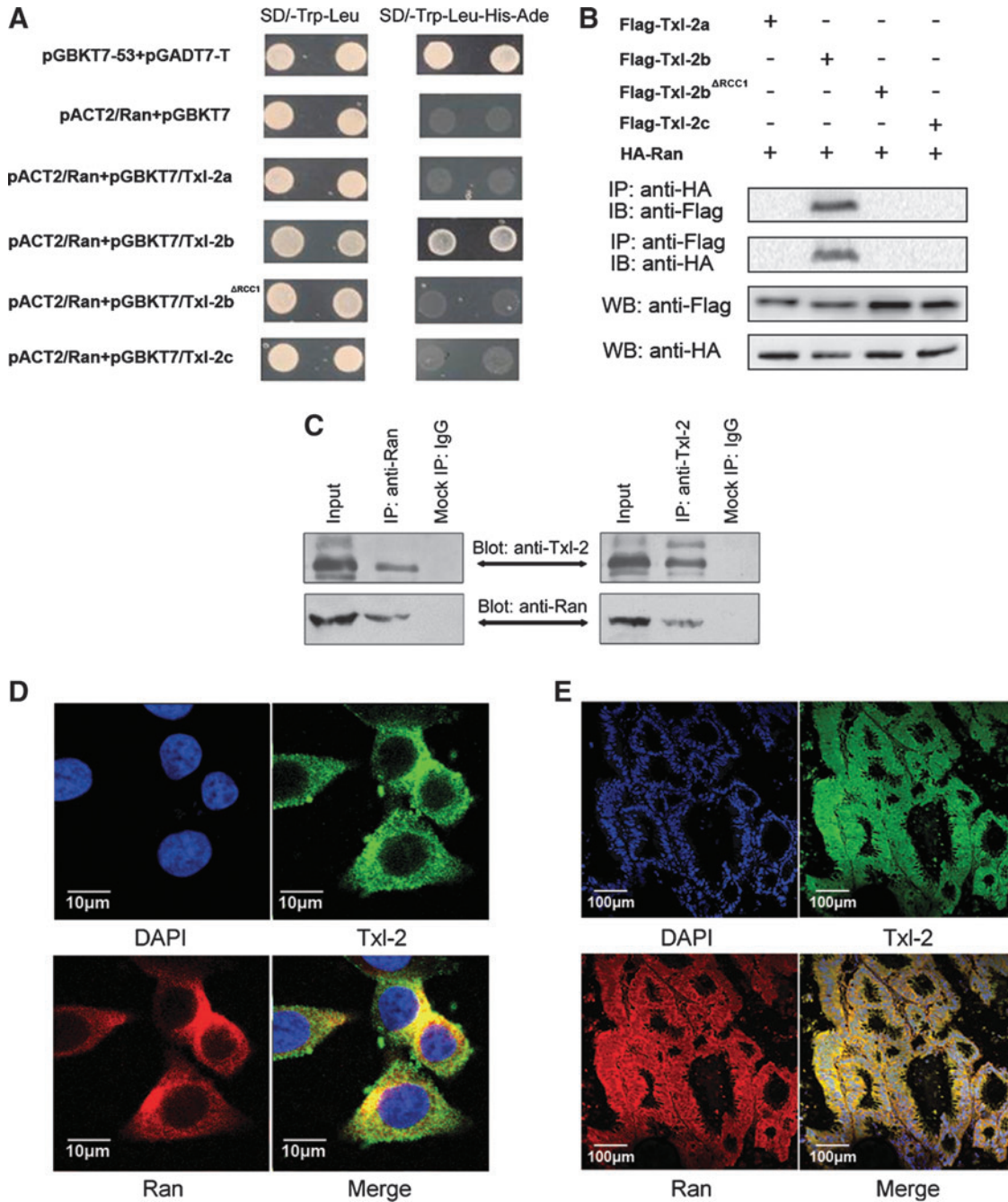


**FIG. 5. Txl-2b interacts with the small GTPase Ran.** (A) Interactions between Txl-2 isoforms and Ran protein were analyzed by the yeast two-hybrid assay. Coding sequences of three Txl-2 splicing variants or Txl-2b lacking RCC1 signature Txl-2b<sup>ARCC1</sup> were cloned into pGBKT7, and Ran into pACT2, and then cotransformed into AH109 yeast strain. A positive clone indicates an interaction between Txl-2b and Ran similar to that of the positive control (pGBKT7-53 + pGADT7-T), whereas no interaction was detected between Txl-2b<sup>ARCC1</sup> and Ran and the negative control (pACT2/Ran + pGBKT7). (B) Flag-tagged Txl-2 isoforms or Txl-2b<sup>ARCC1</sup> were cotransfected with HA-tagged Ran into 293T cells. The lysate was subjected to co-IP with anti-HA antibody and probed with anti-Flag antibody, or co-IP with anti-Flag and probed with anti-HA. Interaction was detected only between Txl-2b with Ran but not for other combinations. (C) Interaction between Txl-2b and Ran in SW620 cells was further tested by coimmunoprecipitation using anti-Txl-2 and anti-Ran antibodies. (D–E) Colocalization (yellow) between Txl-2b and Ran was examined by double immune-fluorescence staining for Txl-2 (green) and Ran (red) in colon cancer cells (D) and colon cancer tissues (E).

39). We previously found that the dimeric conformation of Txl-2 is maintained by disulfide bonds (37). The fact that an intact redox active site in the Trx domain is essential for Txl-2b induced metastasis demonstrates that Txl-2b may function in cancer cell metastasis in a redox-dependent manner. Never-

theless, we still cannot rule out the possibility of the NDPk domain playing a role in the prometastatic effect of Txl-2b since many reports suggest that the histidine protein kinase activity cannot fully explain the functions of NDPk family members in cancer (2, 45).



TABLE 3. CORRELATION ANALYSIS OF THIOREDOXIN-LIKE PROTEIN 2 AND RAN EXPRESSION

		Txl-2		<i>p</i> <sup>a</sup> value
		Negative	Positive	
Ran	Negative	3	3	<0.001
	Positive	1	43	

A paired immunohistochemical study for Txl-2 and Ran expression in 50 cases of colon cancer tissues.

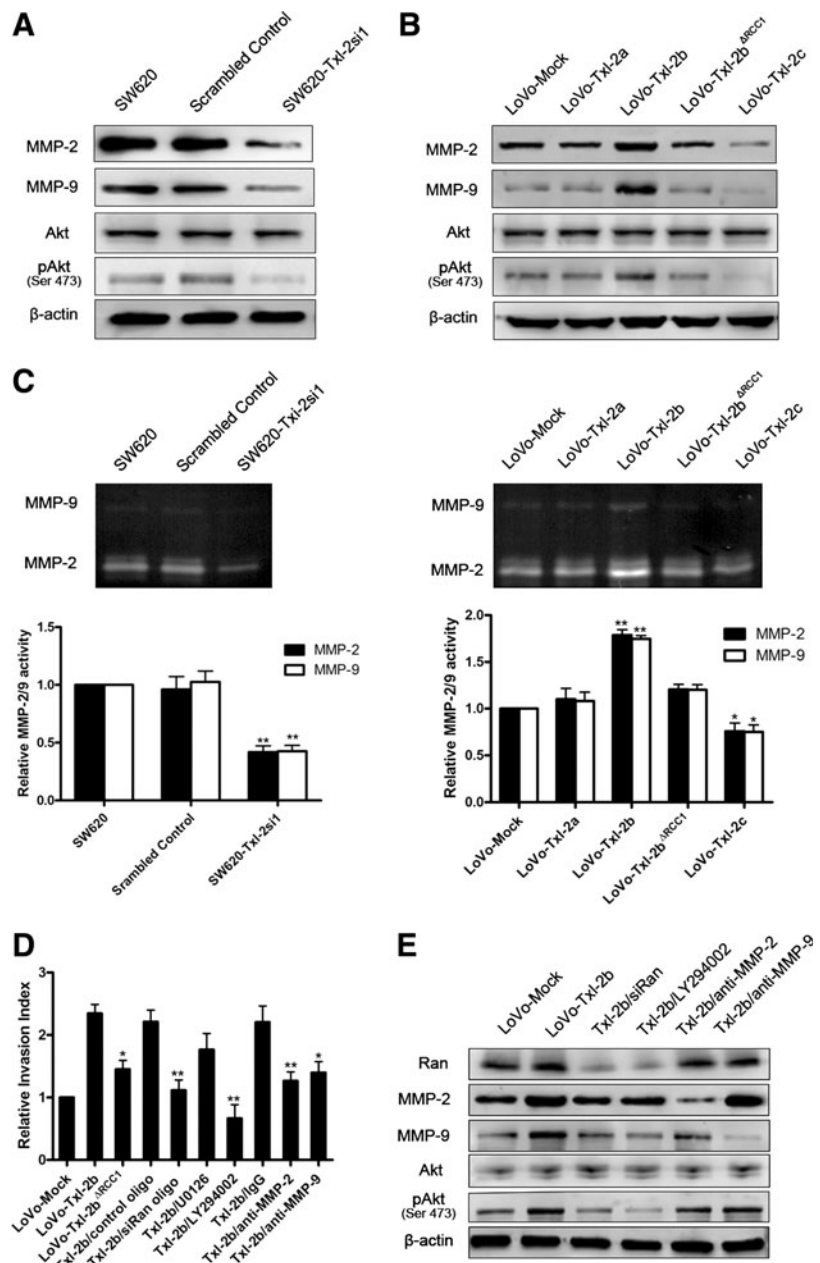
<sup>a</sup>By chi-square test.

We further proceeded to explore the downstream events of Txl-2b induced cancer cell invasion and metastasis. Ran, a small GTP-binding protein from the Ras superfamily, is a well-known molecule that regulates mitotic spindle formation (35). Recently, emerging evidence has been reported on

Ran associating with various cancer malignant phenotypes. Activation of the Ran GTPase is subjected to growth factor regulation and can give rise to cellular transformation (26). Ran is an effector of the invasive and metastatic phenotype induced by osteopontin (20) and its overexpression is also associated with local invasion and metastasis in clear cell renal cell carcinoma and epithelial ovarian cancer (1, 3). Our previous study also discovered Ran overexpression in colon cancer (12) and its prometastatic function (unpublished data). In the present study, we found that Txl-2b exerts its proinvasive and metastatic function, at least partially, through its binding to Ran. Among the three isoforms of Txl-2, only Txl-2b binds Ran, as demonstrated by both yeast two-hybrid assay and coimmunoprecipitation. Deletion of RCC1 signature in Txl-2b abolished its interaction with Ran and cancer cells no longer exhibited the enhanced invasive potential, indicating that Txl-2b interacts with Ran *via* its RCC1 domain and that this

FIG. 6. Phospho-Akt mediates Txl-2b-Ran-matrix metalloproteinase (MMP) signaling induced tumor cell invasion.

(A) Knockdown of Txl-2 expression significantly decreased the expression of MMP-2, MMP-9, and Phospho-Akt (Ser 473). (B) Overexpression of Txl-2b-EGFP fusion protein selectively upregulated MMP-2, MMP-9, and Phospho-Akt levels, whereas deletion of the RCC1 signature in Txl-2b precluded such upregulation.  $\beta$ -actin served as a control. (C) MMP-2/9 gelatinase activity in cancer cells with depletion of Txl-2 or overexpression of the different Txl-2 isoforms. MMP-2/9 activity is depicted as relative to that of SW620 or LoVo mock transfected cells. The results are the mean  $\pm$  SEM from three independent experiments. \**p* < 0.05, \*\**p* < 0.01. (D) Induced cell invasion by overexpression of Txl-2b-EGFP fusion protein was significantly blocked by siRNA-Ran, LY294002 (PI3 Kinase inhibitor), and neutralizing antibodies for MMP-2 and MMP-9, but not U0126 (MEK1/2 inhibitor) and negative controls (Control oligo, DMSO and IgG). Deletion of RCC1 signature also abolished the Txl-2b induced cell invasion. The results are the mean  $\pm$  SEM from three independent experiments. \**p* < 0.05, \*\**p* < 0.01. (E) MMP-9, Phospho-Akt (Ser 473), and total Akt levels were examined by Western blot in LoVo cells overexpressing Txl-2b-EGFP after treatment with siRan, LY294002, anti-MMP-2, and anti-MMP-9.



interaction is critical for colon cancer cell metastasis. Additionally, inhibition of Ran expression by siRNA oligo also blocked Txl-2b mediated tumor cell invasion and metastasis.

It is not clear why Txl-2b is the only isoform that interacts with Ran. The dimeric conformation of Txl-2 is maintained by disulfide bonds (37) and, therefore, it is reasonable to speculate that Txl-2 could be organized as either homodimer or heterodimer composed by different combinations of the various splicing variants. It is possible then that only homodimers composed by Txl-2b isoforms acquire the necessary spatial conformation to interact with Ran, while homodimers of other splicing variants as well as heterodimers are organized in a different spatial conformation; thus, precluding the interaction with Ran. For instance, the feedback regulatory mechanism proposed above for the Txl-2c inhibitory function in metastasis, could be explained by a possible interference of the Txl-2c hetero/homodimers with Txl-2b and Ran or other effectors. Further studies are required to validate this hypothesis.

Similar to Ras and Rho GTPases, exchange of GDP for GTP leads to a conformational change in the Ran GTPase that greatly enhances affinity to downstream effectors (35). In particular, GEFs facilitate exchange of GDP with GTP to promote GTPase activation (34). It is noteworthy that similar to the action of GEFs, redox agents have been shown to stimulate Ran guanine nucleotide dissociation, which results in an increased rate of GDP-GTP exchange and an accelerated activation of Ran function (17, 18). Besides redox regulation of Ran, growing evidence indicates that NDPk family members also interact with Ras-related family members and influence malignant cancer phenotypes (10, 16, 28, 42). In this context, it is tempting to speculate that Txl-2 acts as a GEF to Ran in a redox-dependent manner and facilitates Ran activity and the downstream effectors, maybe also aided by its NDPk domain.

MMPs belong to a family of enzymes that degrade the extracellular matrix components and, therefore, play an important role in tissue repair, tumor invasion, and metastasis. There is evidence that Trx family members can regulate MMP expression and stimulate tumor cell invasion (13, 31). MMP-2 and MMP-9 are the most important proteases for the degradation of the main constituents of the basement membrane, type IV collagen. Importantly, upregulation of MMP-2 and MMP-9 accelerates cell migration and invasion in CRC (29). In our study, MMP-2 and MMP-9 expression and activity were upregulated in Txl-2b overexpressing cells, accompanied by increased levels of phosphorylated AKT. However, no significant changes were detected in cells overexpressing the deletion mutant Txl-2b<sup>ΔRCC1</sup>, suggesting that MMP-2 and MMP-9 might be regulated by the interaction between Txl-2b and Ran.

Interactions between different transcription factors provide fine-tuning of the transcriptional regulation of MMP promoter activity. The expression of most MMPs members, including MMP-2 and MMP-9, has been shown to be regulated by activator protein 1 (AP-1) and nuclear factor- $\kappa$ B (NF- $\kappa$ B) (8, 14). Interestingly, many Trx family members regulate the DNA-binding activity of transcription factors, such as AP-1, NF- $\kappa$ B, and p53 (23, 33, 39). Besides, NF- $\kappa$ B and AP-1 can also be regulated by some members of the NDP kinase family, such as Nm23-H2 and Nm23-H5 (21, 22). Indeed, we have found increased phosphorylation of the NF- $\kappa$ B kinase IKK in Txl-2b overexpressing cells (unpublished data). It is then possible that Txl-2b, through modulating NF- $\kappa$ B or AP-1 transcriptional activities, induces MMP-2 and MMP-9 gene

expression. Dysregulation of PI3K/Akt pathway plays an essential role in cancer development (44). Akt activation was found through Txl-2b and Ran interaction. Since NF- $\kappa$ B and AP-1 are the downstream targets of PI3K/Akt (44), and Akt can also be a downstream target of NF- $\kappa$ B (27), further studies are ongoing to explore the interplay between them.

In summary, our data demonstrate that Txl-2 is overexpressed in colon cancer and its levels correlate with cancer progression, providing evidence that Txl-2 may be a novel effector of invasion and metastasis in colon cancer. Based on our findings, we propose a mechanism by which the splicing variant Txl-2b mediates tumor invasion and metastasis through directly interaction with Ran *via* PI3K pathway and modulation of MMP-2/9 expression. Inhibition of the Txl-2b-Ran-MMP signaling arises as an attractive target for colon cancer therapy. In normal tissues, Txl-2 is mainly expressed in testis and this work demonstrates that dysregulated expression of Txl-2 promotes cancer progression; thus, categorizing Txl-2 as a putative novel cancer-testis antigen. Cancer-testis antigens are potentially suitable targets for tumor vaccines because of their high immunogenicity *in vivo*, even in cancer-bearing patients, and their restricted normal tissue distribution (24). Therefore, our data provide a novel biomarker and a target molecule for the diagnosis and treatment of colon cancer.

## Materials and Methods

### Cell culture and transfection

Human colon adenocarcinoma cell lines SW480, LoVo and human 293T cells were preserved by our institute. Cells were cultured in RPMI 1640 medium (Invitrogen, Carlsbad, CA) supplemented with 10% fetal bovine serum (Hyclone, Logan, UT), 100  $\mu$ /ml penicillin, and 100  $\mu$ g/ml streptomycin (Sigma-Aldrich, St Louis, MO) at 37°C with a humidified atmosphere of 95% air and 5% CO<sub>2</sub>. Cell transfection was performed with Lipofectamine<sup>TM</sup> 2000 (Invitrogen) as described in the manufacturer's protocol.

### Antibodies and reagents

The rabbit anti-Txl-2 polyclonal antibody able to recognize the three isoforms was produced by us previously (37). Goat polyclonal anti-Ran antibody was from Santa Cruz Biotechnology (Santa Cruz, CA). Anti-MMPs antibodies, phospho-Akt pathway antibody sampler kit, PI3 Kinase inhibitor LY294002, and the MEK1/2 inhibitor U0126 were from Cell Signaling Technology (Beverly, MA). Protein A/G agarose was obtained from Calbiochem (Cambridge, MA). Anti-GFP antibody was obtained from eBioscience (San Diego, CA). Anti-Flag and anti-HA antibodies were from Santa Cruz Biotechnology. Anti- $\beta$ -actin antibody was from Sigma-Aldrich.

### Tissue collection

Formalin-fixed, paraffin-embedded tumor tissue, and corresponding normal tissue blocks were collected from 243 colon cancer patients who underwent surgical resection during 2004 in the Department of Pathology at the Tianjin Union Medicine Centre, China. All cases of colon cancer and adjacent non-tumorous tissues were diagnosed clinically and pathologically. This study was approved by the Ethics Committee of Tianjin Union Medicine Centre. Enrolled patients were followed up at least 5 years for survival calculations.

### Immunohistochemical staining

Txl-2 immunostaining was performed by an avidin-biotin method as described previously (25). The expression of Txl-2 was determined by assessing the percentage of decorated tumor cells and the staining intensity semiquantitatively. The percentage of positive cells was rated as follows: 0 (no cells), 1 (1%–25%), 2 (26%–50%), 3 (51%–75%), or 4 (76%–100%). The staining intensity was rated as follows: 0, no signal; 1, weak; 2, moderate; and 3, strong staining. A total score of 0–12 was then calculated and graded as I: score 0 and 1, II: 2, 3 and 4, III: 6 and 8, and IV: 9 and 12.

### RNA preparation and semiquantitative RT-PCR

Fifty cases of fresh colon cancer samples were collected, including the adjacent normal tissues. mRNA was prepared using Trizol (Invitrogen) according to the manufacturer's instructions. Semiquantitative RT-PCR and the quantification were performed as previously described (25).

### Plasmid construction

pSilencer3.1-H1 (Ambion, Austin, TX) was used for construction of human Txl-2 siRNA expression vectors pSilencer Txl-2 #1 and #2 according to the manufacturer's protocol. The open reading frame of human full-length Txl-2 and Txl-2b were cloned into pGEX-4T-1 expression vector as previously described (37). The products were then subcloned into the vector pEGFP-N3 (BD Biosciences Clontech). cDNA of Txl-2c was obtained by two-step overlapping PCR using two sets primers. For generation of vectors with mutated Txl-2b, cysteine residues in the active site of Trx domain were replaced with serine residues (Cys->Ser) in pEGFP-N3-Txl-2b<sup>CS</sup>, while in pEGFP-N3-Txl-2b<sup>HP</sup>, the histidine residue in the active site of NDPk domain was replaced with proline (His->Pro). Double mutant vector of both active sites in Trx and NDPk domain was also generated using the above described mutations and named pEGFP-N3-Txl-2b<sup>DM</sup>. These site-specific mutations were conducted by PCR using three primer sets. The RCC1 signature (MCSGPSHLLIL) between residues 161 and 171 of Txl-2b was deleted to generate the pEGFP-N3-Txl-2b<sup>ARCC1</sup> by PCR. All the primers used in this section are listed in Supplementary Table S1. All the constructs were verified by sequencing in both directions.

### Invasion assay

Cell invasion assays were performed using Transwells (8 mm pore size; Corning Costar Corp., Acton, MA) as previously described (20). In some cases, inhibitors or MMP-2 or MMP-9 antibodies (10 µg/ml; Cell Signaling Technology) were also added to the upper and lower chambers.

### Soft agar colonization assay

Cells were plated in triplicate in a 24-well plate at  $5 \times 10^3$  cells/well, as previously described (20). All colonies composed of greater than 50 cells were counted in each well using a digital imaging system (Olympus Corp., Tokyo, Japan).

### Immunoprecipitation

Cells were lysed in a buffer containing 150 mM NaCl, 25 mM Tris-HCl, pH 7.45, 0.5% Nonidet P-40, 0.1% sodium dodecyl

sulfate (SDS), 1 mM dithiothreitol, 0.2 mM phenylmethylsulfonyl fluoride (pH 7.5), and a protease inhibitor cocktail. Cell lysates were precleared with agarose beads for 2 h at 4°C and mixed with anti-Txl-2, or anti-Ran-coated protein A/G agarose overnight at 4°C. The agarose was extensively washed with a high-stringency wash buffer containing 0.1% SDS, and the associated proteins were stored for further immunoblot analysis.

### Yeast two-hybrid assay

Yeast two-hybrid assay was done using the Matchmaker System (Clontech, Palo Alto, CA) following the manufacturer's protocols. Full-length Ran cDNAs were cloned into the pACT2 plasmid (Clontech) where they were expressed as fusion proteins to the GAL4 activation domain. For the bait protein, Txl-2a, b, and c cDNA and the deletion mutant Txl-2b<sup>ARCC1</sup> were cloned into the pGBKT7 plasmid, respectively, and expressed as a fusion to GAL4 DNA binding domain. Plasmids were cotransformed into AH109 yeast strain and positive clones were observed on high-stringency dropout plates (-Leu/-Trp/-His/-Ade).

### Immunofluorescence staining

Cells were plated onto glass coverslips and fixed with 4% paraformaldehyde for 20 min and permeabilized with 0.1% Triton X-100 in phosphate-buffered saline for 15 min. Blocking solution was applied for 1 h at room temperature. Rabbit polyclonal anti-Txl-2 antibody (1:150) and goat polyclonal anti-Ran antibody (1:200) were applied at 4°C overnight. FITC-conjugated and Cy3-conjugated secondary antibodies were loaded and incubated for 2 h at room temperature. Immunostaining signal and DAPI-stained nuclei were visualized by the FLUOVIEW laser scanning confocal microscope (Olympus Corp.).

### Gelatin zymography

The enzymatic activity of MMP-2 and MMP-9 was determined using a gelatin zymography assay kit (GENMED Scientifics, Inc., Shanghai, China), as described previously (43). In brief, the conditioned medium containing equal amounts of protein was separated on a 10% SDS-polyacrylamide gel electrophoresis containing 0.1% gelatin. Gels were placed in 2.5% Triton X-100 for 30 min, incubated for 24 h in buffer (50 mM Tris-HCl, pH 7.4, 5 mM CaCl<sub>2</sub>) and stained with Coomassie blue R-250.

### Tail vein metastatic assay

Every experimental group had eighteen 4 to 6-week-old BALB/C-nu/nu nude mice obtained from the Shanghai Laboratory Animal Center of China. Each mouse was injected *via* tail vein with  $2.5 \times 10^6$  cells. Four weeks later, 8 mice were sacrificed, and 4 µM paraffin-embedded sections of lung and liver tissues were prepared. The sections were stained with hematoxylin and eosin and examined for the presence of metastatic tumor foci under microscopy. The rest of the mice ( $n = 10$  per group) were maintained for survival analysis and studied until they were dead.

### Statistical analysis

All statistical analyses were performed using SPSS16.0 software (Chicago, IL). Mann-Whitney U-test for two groups

and Kruskal–Wallis H-test for multigroups were used in the analysis of immunohistochemical results. Survival was assessed by the Kaplan–Meier method and statistical analysis performed by Log-Rank testing. Numerical data are presented as the mean  $\pm$  SEM. The differences between groups were analyzed using the Student's *t*-test when comparing only two groups or assessed by one-way analysis of variance when more than two groups were compared.  $p < 0.05$  was considered as statistically significant.

### Acknowledgments

We thank Prof. Peisong Gao (Division of Allergy and Clinical Immunology, Department of Medicine, the Johns Hopkins University) and Prof. Jianping Jin (Department of Physiology, Wayne State University School of Medicine) for their contribution to the preparation of this manuscript. We also thank Yunmin Li (Department of Health Statistics, The Fourth Military Medical University, China) for his assistance in statistical analysis. This work was supported by grants from National Key Basic Research and Development Program (2010CB529300, 2009CB521805, 2010CB529306) and National Science Foundation of China (NSF: 81201929, 30971337, 81272650).

### Author Disclosure Statement

No competing financial interests exist.

### References

1. Abe H, Kamai T, Shirataki H, Oyama T, Arai K, and Yoshida K. High expression of Ran GTPase is associated with local invasion and metastasis of human clear cell renal cell carcinoma. *Int J Cancer* 122: 2391–2397, 2008.
2. Almgren MA, Henriksson KC, Fujimoto J, and Chang CL. Nucleoside diphosphate kinase A/nm23-H1 promotes metastasis of NB69-derived human neuroblastoma. *Mol Cancer Res* 2: 387–394, 2004.
3. Barres V, Ouellet V, Lafontaine J, Tonin PN, Provencher DM, and Mes-Masson AM. An essential role for Ran GTPase in epithelial ovarian cancer cell survival. *Mol Cancer* 9: 272, 2010.
4. Bilitou A, Watson J, Gartner A, and Ohnuma S. The NM23 family in development. *Mol Cell Biochem* 329: 17–33, 2009.
5. Boissan M, Dabernat S, Peuchant E, Schlattner U, Lascu I, and Lacombe ML. The mammalian Nm23/NDPK family: from metastasis control to cilia movement. *Mol Cell Biochem* 329: 51–62, 2009.
6. Brown RL, Reinke LM, Damerow MS, Perez D, Chodosh LA, Yang J, and Cheng C. CD44 splice isoform switching in human and mouse epithelium is essential for epithelial-mesenchymal transition and breast cancer progression. *J Clin Invest* 121: 1064–1074, 2011.
7. Center MM, Jemal A, Smith RA, and Ward E. Worldwide variations in colorectal cancer. *CA Cancer J Clin* 59: 366–378, 2009.
8. Chakraborti S, Mandal M, Das S, Mandal A, and Chakraborti T. Regulation of matrix metalloproteinases: an overview. *Mol Cell Biochem* 253: 269–285, 2003.
9. Christensen B, Klaning E, Nielsen MS, Andersen MH, and Sorensen ES. C-terminal modification of osteopontin inhibits interaction with the  $\alpha$ V $\beta$ 3-integrin. *J Biol Chem* 287: 3788–3797, 2012.
10. Conery AR, Sever S and Harlow E. Nucleoside diphosphate kinase Nm23-H1 regulates chromosomal stability by activating the GTPase dynamin during cytokinesis. *Proc Natl Acad Sci U S A* 107: 15461–15466, 2010.
11. Deschoolmeester V, Baay M, Specenier P, Lardon F, and Vermorken JB. A review of the most promising biomarkers in colorectal cancer: one step closer to targeted therapy. *Oncologist* 15: 699–731, 2010.
12. Fan H, Lu Y, Qin H, Zhou Y, Gu Y, Zhou J, Wang X, and Fan D. High Ran level is correlated with poor prognosis in patients with colorectal cancer. *Int J Clin Oncol* 2012. [Epub ahead of print]; DOI: 10.1007/s10147-012-0465-x.
13. Farina AR, Tacconelli A, Cappabianca L, Masciulli MP, Holmgren A, Beckett GJ, Gulino A, and Mackay AR. Thioredoxin alters the matrix metalloproteinase/tissue inhibitors of metalloproteinase balance and stimulates human SK-N-SH neuroblastoma cell invasion. *Eur J Biochem* 268: 405–413, 2001.
14. Gialeli C, Theocharis AD and Karamanos NK. Roles of matrix metalloproteinases in cancer progression and their pharmacological targeting. *FEBS J* 278: 16–27, 2011.
15. Hall A. The cytoskeleton and cancer. *Cancer Metastasis Rev* 28: 5–14, 2009.
16. Hartsough MT, Morrison DK, Salerno M, Palmieri D, Ouatas T, Mair M, Patrick J, and Steeg PS. Nm23-H1 metastasis suppressor phosphorylation of kinase suppressor of Ras via a histidine protein kinase pathway. *J Biol Chem* 277: 32389–32399, 2002.
17. Heo J. Redox control of GTPases: from molecular mechanisms to functional significance in health and disease. *Antioxid Redox Signal* 14: 689–724, 2011.
18. Heo J. Redox regulation of Ran GTPase. *Biochem Biophys Res Commun* 376: 568–572, 2008.
19. Kubens BS and Zanker KS. Differences in the migration capacity of primary human colon carcinoma cells (SW480) and their lymph node metastatic derivatives (SW620). *Cancer Lett* 131: 55–64, 1998.
20. Kurisetty VV, Johnston PG, Johnston N, Erwin P, Crowe P, Fernig DG, Campbell FC, Anderson IP, Rudland PS, and El-Tanani MK. RAN GTPase is an effector of the invasive/metastatic phenotype induced by osteopontin. *Oncogene* 27: 7139–7149, 2008.
21. Lee MJ, Xu DY, Li H, Yu GR, Leem SH, Chu IS, Kim IH, and Kim DG. Pro-oncogenic potential of NM23-H2 in hepatocellular carcinoma. *Exp Mol Med* 44: 214–224, 2012.
22. Li F, Hu G, Jiang Z, Guo J, Wang K, Ouyang K, Wen D, Zhu M, Liang J, Qin X, and Zhang L. Identification of NME5 as a contributor to innate resistance to gemcitabine in pancreatic cancer cells. *FEBS J* 279: 1261–1273, 2012.
23. Lillig CH and Holmgren A. Thioredoxin and related molecules—from biology to health and disease. *Antioxid Redox Signal* 9: 25–47, 2007.
24. Lim SH, Zhang Y and Zhang J. Cancer-testis antigens: the current status on antigen regulation and potential clinical use. *Am J Blood Res* 2: 29–35, 2012.
25. Lu Y, Wang X, Liu Z, Jin B, Chu D, Zhai H, Zhang F, Li K, Ren G, Miranda-Vizuete A, Guo X, and Fan D. Identification and distribution of thioredoxin-like 2 as the antigen for the monoclonal antibody MC3 specific to colorectal cancer. *Proteomics* 8: 2220–2229, 2008.
26. Ly TK, Wang J, Pereira R, Rojas KS, Peng X, Feng Q, Cerione RA, and Wilson KF. Activation of the Ran GTPase is subject to growth factor regulation and can give rise to cellular transformation. *J Biol Chem* 285: 5815–5826, 2010.
27. Meng F, Liu L, Chin PC, and D'Mello SR. Akt is a downstream target of NF-kappa B. *J Biol Chem* 277: 29674–29680, 2002.

28. Miyamoto M, Iwashita S, Yamaguchi S, and Ono Y. Role of nm23 in the regulation of cell shape and migration via Rho family GTPase signals. *Mol Cell Biochem* 329: 175–179, 2009.
29. Mook OR, Frederiks WM and Van Noorden CJ. The role of gelatinases in colorectal cancer progression and metastasis. *Biochim Biophys Acta* 1705: 69–89, 2004.
30. Noike T, Miwa S, Soeda J, Kobayashi A, and Miyagawa S. Increased expression of thioredoxin-1, vascular endothelial growth factor, and redox factor-1 is associated with poor prognosis in patients with liver metastasis from colorectal cancer. *Hum Pathol* 39: 201–208, 2008.
31. Oh JH, Chung AS, Steinbrenner H, Sies H, and Brenneisen P. Thioredoxin secreted upon ultraviolet A irradiation modulates activities of matrix metalloproteinase-2 and tissue inhibitor of metalloproteinase-2 in human dermal fibroblasts. *Arch Biochem Biophys* 423: 218–226, 2004.
32. Pajares MJ, Ezponda T, Catena R, Calvo A, Pio R, and Montuenga LM. Alternative splicing: an emerging topic in molecular and clinical oncology. *Lancet Oncol* 8: 349–357, 2007.
33. Qu Y, Wang J, Ray PS, Guo H, Huang J, Shin-Sim M, Bukoye BA, Liu B, Lee AV, Lin X, Huang P, Martens JW, Giuliano AE, Zhang N, Cheng NH, and Cui X. Thioredoxin-like 2 regulates human cancer cell growth and metastasis via redox homeostasis and NF-kappaB signaling. *J Clin Invest* 121: 212–225, 2011.
34. Renault L, Kuhlmann J, Henkel A, and Wittinghofer A. Structural basis for guanine nucleotide exchange on Ran by the regulator of chromosome condensation (RCC1). *Cell* 105: 245–255, 2001.
35. Rensen WM, Mangiacasale R, Ciciarello M, and Lavia P. The GTPase Ran: regulation of cell life and potential roles in cell transformation. *Front Biosci* 13: 4097–4121, 2008.
36. Rundlof AK, Fernandes AP, Selenius M, Babic M, Shariatgorji M, Nilsson G, Ilag LL, Dobra K, and Bjornstedt M. Quantification of alternative mRNA species and identification of thioredoxin reductase 1 isoforms in human tumor cells. *Differentiation* 75: 123–132, 2007.
37. Sadek CM, Jimenez A, Damdimopoulos AE, Kieselbach T, Nord M, Gustafsson JA, Spyrou G, Davis EC, Oko R, van der Hoorn FA, and Miranda-Vizuete A. Characterization of human thioredoxin-like 2. A novel microtubule-binding thioredoxin expressed predominantly in the cilia of lung airway epithelium and spermatid manchette and axoneme. *J Biol Chem* 278: 13133–13142, 2003.
38. Seifert M, Welter C, Mehraein Y, and Seitz G. Expression of the nm23 homologues nm23-H4, nm23-H6, and nm23-H7 in human gastric and colon cancer. *J Pathol* 205: 623–632, 2005.
39. Shlomai J. Redox control of protein-DNA interactions: from molecular mechanisms to significance in signal transduction, gene expression, and DNA replication. *Antioxid Redox Signal* 13: 1429–1476, 2010.
40. Sigrist CJ, Cerutti L, de Castro E, Langendijk-Genevaux PS, Bulliard V, Bairoch A, and Hulo N. PROSITE, a protein domain database for functional characterization and annotation. *Nucleic Acids Res* 38: D161–D166, 2010.
41. Speletas M, Argentou N, Karanikas V, Gramoustianou ES, Mandala E, Braimi M, Matsouka P, Ritis K, and Germenis AE. Survivin isoform expression patterns in CML patients correlate with resistance to imatinib and progression, but do not trigger cytolytic responses. *Clin Immunol* 139: 155–163, 2011.
42. Tseng YH, Vicent D, Zhu J, Niu Y, Adeyinka A, Moyers JS, Watson PH, and Kahn CR. Regulation of growth and tumorigenicity of breast cancer cells by the low molecular weight GTPase Rad and nm23. *Cancer Res* 61: 2071–2079, 2001.
43. Wang J, Zhou X, Cui L, Yan L, Liang J, Cheng X, Qiao L, Shi Y, Han Z, Cao Y, Han Y, and Fan D. The significance of CD14+ monocytes in peripheral blood stem cells for the treatment of rat liver cirrhosis. *Cytotherapy* 12: 1022–1034, 2010.
44. Zhang X, Jin B and Huang C. The PI3K/Akt pathway and its downstream transcriptional factors as targets for chemoprevention. *Curr Cancer Drug Targets* 7: 305–316, 2007.
45. Zhou Q, Yang X, Zhu D, Ma L, Zhu W, Sun Z, and Yang Q. Double mutant P96S/S120G of Nm23-H1 abrogates its NDPK activity and motility-suppressive ability. *Biochem Biophys Res Commun* 356: 348–353, 2007.

#### Abbreviations Used

AP-1 = activator protein 1
CRC = colorectal cancer
GEF = guanine nucleotide exchange factor
HR = hazard ratio
MMP = matrix metalloproteinase
NDPK = nucleoside-diphosphate kinase
NF-κB = nuclear factor-κB
PCR = polymerase chain reaction
RCC1 = regulator of chromosome condensation-1
RT-PCR = reverse transcription polymerase chain reaction
SDS = sodium dodecyl sulfate
Txl-2 = thioredoxin-like protein 2
Trx = thioredoxin

Address correspondence to:

Dr. Daiming Fan  
State Key Laboratory of Cancer Biology  
Xijing Hospital of Digestive Diseases  
Fourth Military Medical University  
127# Changle West Road  
Xi'an 710032  
China

E-mail: daimingfan@yahoo.cn

Dr. Xin Wang  
State Key Laboratory of Cancer Biology  
Xijing Hospital of Digestive Diseases  
Fourth Military Medical University  
127# Changle West Road  
Xi'an 710032  
China

E-mail: wangx@fmmu.edu.cn

Dr. Antonio Miranda-Vizuete  
Instituto de Biomedicina de Sevilla (IBiS)  
Hospital Universitario Virgen del Rocío/CSIC/  
Universidad de Sevilla  
Laboratorio 118  
Avda. Manuel Siurot s/n  
Seville 41013  
Spain

E-mail: amiranda-ibis@us.es

Date of first submission to ARS Central, June 3, 2012; date of final revised submission, December 18, 2012; date of acceptance, January 11, 2013.